Volume 19, Number 3, 2026. pp. 403-408

Jordan Journal of Physics

ARTICLE

Modeling Coherence Length Anisotropy in High-T_c Superconductors Using a Paraconductivity Approach

M. A. Islam and **M. R. Islam**

Department of Physics, University of Chittagong, Chattogram-4331, Bangladesh.

DOI: **https://doi.org/10.47011/19.3.11**

Received on: 18/09/2025; *Accepted on: 26/11/2025*

Abstract: We present a theoretical framework to estimate the coherence length anisotropy in high-temperature superconductors. A detailed analysis is carried out using the paraconductivity approach and is compared with the available experimental data. The theoretical model is developed based on the established paraconductivity expressions for anisotropic superconductors. Numerical evaluations have been performed for the superconducting $(ZnO)_x$/(Bi,Pb)-2223 and $(Ti)_x$/(Cu,Tl)-1223 phases. The theoretical predictions agree better with the experimental results for these materials, supporting the validity of the proposed model.

Keywords: High-temperature superconductor, Anisotropy, Paraconductivity.

1. Introduction

Anisotropy is a key concept in both the theoretical modeling and practical utilization of superconducting materials. It influences how researchers interpret experimental observations and how superconductors perform in technological applications. Depending on the context, anisotropy may be viewed as a subject of fundamental scientific interest [1–6], an undesirable feature that limits performance [7], or a tunable property that can be optimized for specific functions [8, 9]. Generally, two main factors contribute to anisotropic behavior: (i) the intrinsic anisotropy arising from the crystal structure and electronic properties of the material, and (ii) the pinning anisotropy associated with directional variations in vortex pinning mechanisms.

High-Temperature SuperConductors (HTSCs) are well known for their strong anisotropy, short coherence lengths, and relatively high critical temperatures (T_c) [10]. Many of the recently developed oxide-based superconductors exhibit pronounced anisotropy, primarily due to their layered crystal structures. As a result, their physical and electronic properties vary along the three crystallographic axes (*a*, *b*, and *c*) or equivalently (*x*, *y*, and *z*).

Coherence length anisotropy occurs when superconducting properties differ along these axes. In layered superconductors, superconductivity is typically stronger within the planes (the *ab*-plane) than between the planes (along the *c*-axis). The difference between the *a*- and *b*-directions is often small enough to be neglected, leading to the assumption of axial symmetry where '*a*' = '*b*'. Under this condition, the coherence lengths are expressed as $\xi_a(0) = \xi_b(0) \approx \xi_{ab}(0) \neq \xi_c(0)$, or equivalently $\xi_x(0) = \xi_y(0) \approx \xi_{xy}(0) \neq \xi_z(0)$. The ratio $\gamma = \xi_{ab}/\xi_c = \xi_{xy}/\xi_z$ defines the anisotropy parameter (γ), also referred to as the anisotropy ratio or anisotropic coefficient.

Determining γ is crucial for both fundamental research in superconductivity and for practical design considerations [11, 12]. It provides insights into the electronic structure of the material, such as Fermi surface topology and superconducting gap characteristics. From an applications perspective, a smaller anisotropy parameter is beneficial because it enhances the critical current density in the presence of

Corresponding Author: M. A. Islam **Email**: ashadphysics@gmail.com

magnetic fields by reducing flux cutting and minimizing thermal fluctuations [13].

2. Theoretical Model

The excess dc conductivity, or paraconductivity, due to thermal fluctuations (in a zero magnetic field) was first calculated by Aslamazov and Larkin (A-L) [14], using microscopic theory valid for isotropic low- as well as high-temperature superconductors. Following Aslamazov and Larkin, Hopfengärtner and co-workers [15] obtained the following expression for the excess dc conductivity tensor of anisotropic high-temperature superconductors:

$$\Delta\sigma_{\alpha\beta}(\mathrm{T}) = \frac{e^2\pi\xi_\alpha^2(0)\xi_\beta^2(0)}{\hbar V\varepsilon^3(\mathrm{T})}\sum_{\mathrm{K}}\frac{K_\alpha K_\beta}{\left[1+\xi_x^2(\mathrm{T})K_x^2+\xi_y^2(\mathrm{T})K_y^2+\xi_z^2(\mathrm{T})K_z^2\right]^3}. \quad (1)$$

Here, $\xi_{\alpha,\beta}(\mathrm{T})$ denotes the anisotropic coherence length $(\alpha, \beta = x, y, z)$ and V is the sample volume. For an anisotropic system, one can assume that $\xi_x(0) = \xi_y(0) \neq \xi_{xy}(0)$ (equivalence of in-plane coherence length for layered superconductors) and introduce a factor γ_1 [16]:

$$\xi_{xy}(0) = \gamma_1\xi_z(0), \quad (2)$$

where $\gamma_1[\equiv \xi_{xy}/\xi_z]$ is a ratio, called the coherence length anisotropy ratio, to be determined for specific superconducting samples.

Using relation (2) and substituting $\xi_z(\mathrm{T}) = \xi_z(0)\varepsilon^{-1/2}$, $\varepsilon = (\mathrm{T} - \mathrm{T_c})/\mathrm{T_c}$; Eq. (1) takes the form:

$$\Delta\sigma_{xx}(\mathrm{T}) = \frac{e^2\pi\gamma_1^4\xi_z^4(\mathrm{T})}{\hbar V\varepsilon(\mathrm{T})}\sum_{\mathrm{K}}\frac{K_x^2}{\left[1+(2\gamma_1^2+1)\xi_z^2(\mathrm{T})K_x^2\right]^3}. \quad (3)$$

To evaluate $\Delta\sigma$ for different dimensions, we replace the sum with an appropriate integration. Comparing with the standard integrals [17] and performing the integration, the final results for paraconductivity in different dimensions are as follows [16]:

$$\Delta\sigma^{3\mathrm{D}}(\mathrm{T}) = \gamma\frac{e^2}{32\hbar\xi_z(0)}\varepsilon^{-1/2},$$

$$\gamma = \gamma_1^4\left\{\left(1+2\gamma_1^2\right)/3\right\}^{-5/2} \quad (4)$$

$$\Delta\sigma^{2\mathrm{D}}(\mathrm{T}) = \gamma'\left(\frac{4}{9}\right)\frac{e^2}{16\hbar d}\varepsilon^{-1},$$

$$\gamma' = 9\gamma_1^4\left\{\left(1+2\gamma_1^2\right)/3\right\}^{-2} \quad (5)$$

$$\Delta\sigma^{1\mathrm{D}}(\mathrm{T}) = \gamma''\left(\frac{1}{3\sqrt{3}}\right)\frac{e^2\pi\xi_z(0)}{32\hbar s}\varepsilon^{-3/2},$$

$$\gamma'' = \gamma_1^4\left\{\left(1+2\gamma_1^2\right)/3\right\}^{-3/2}. \quad (6)$$

The general expression for paraconductivity (Eq. (1)) obtained in reference [15] is also valid for isotropic superconductors. For example, a similar calculation yields the same but slightly modified result for paraconductivity:

$$\Delta\sigma^{3\mathrm{D}}(\mathrm{T}) = \frac{e^2}{32\hbar\xi_z(0)}\varepsilon^{-1/2}, \quad (7)$$

$$\Delta\sigma^{2\mathrm{D}}(\mathrm{T}) = \left(\frac{4}{9}\right)\frac{e^2}{16\hbar d}\varepsilon^{-1}, \quad (8)$$

$$\Delta\sigma^{1\mathrm{D}}(\mathrm{T}) = \left(\frac{1}{3\sqrt{3}}\right)\frac{e^2\pi\xi_z(0)}{32\hbar s}\varepsilon^{-3/2}, \quad (9)$$

where we have assumed that $\xi_x = \xi_y = \xi_z \equiv \xi$, $\xi = \left(\xi_x\xi_y\xi_z\right)^{1/3}$.

Thus, we have the modified paraconductivity expressions for an anisotropic superconductor with the constants $\gamma, \gamma', \gamma''$ (corresponding to γ_1). The constant γ_1 is the ratio of the coherence length $(\gamma_1 \equiv \xi_{xy}/\xi_z \equiv \xi_{ab}/\xi_c \equiv \xi_\parallel/\xi_\perp)$, the so-called coherence length anisotropy. If there is no anisotropy, i.e., $\gamma_1 = 1$, the paraconductivity expressions (Eqs. (4), (5) and (6)) for anisotropic systems reduce to the expressions (Eqs. (7), (8), and (9)) for isotropic systems, which proves our assumption.

3. Numerical Results

We have modified paraconductivity expressions for one-, two-, and three-dimensions for anisotropic high-temperature superconductors. Here, our aim is to estimate the anisotropy of the superconducting samples. Although we have derived the one-dimensional paraconductivity expressions theoretically, it is quite impossible to measure the anisotropy of one-dimensional samples experimentally. Therefore, we have to proceed with the two- and three-dimensional paraconductivity expressions for numerical analysis.

It is very interesting to note, that including the parameters $\gamma, \gamma', \gamma''$ (corresponding to γ_1 in Eqs. (4–6)) indicates the limitation of the

anisotropy of the superconducting samples. For larger anisotropy, i.e., for $\gamma_1 >> 1$, Eq. (5) implies $\gamma' \leq 2.25$. Eq. (6) also implies that γ'' is large for very large values of γ_1, indicating higher anisotropy in lower dimensions. But Eq. (4) is a very complicated one from which we cannot determine the maximum value of γ. The numerical results show that at $\gamma_1 = 2$, $\gamma = 1.026$ and tends to zero for larger values of γ_1(Fig. 1).

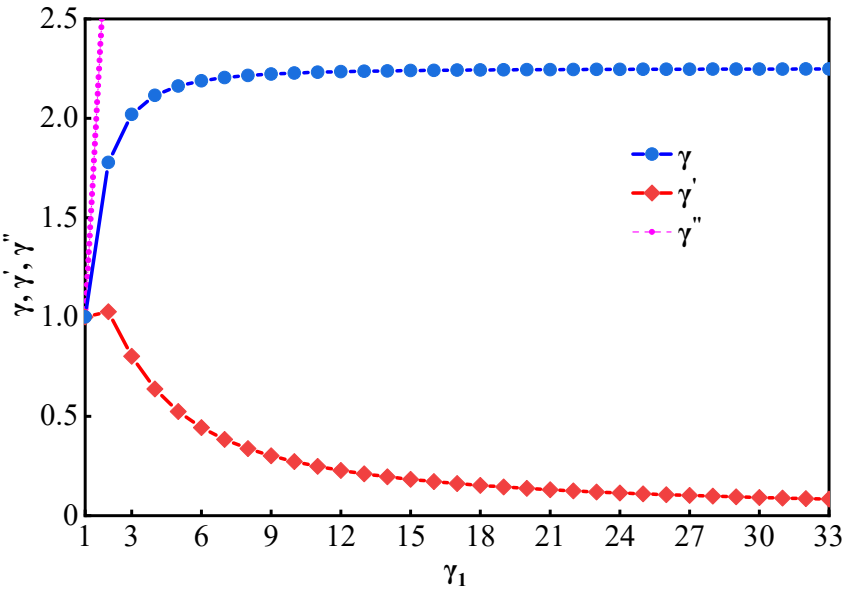

FIG. 1. Variations in $\gamma, \gamma', \gamma''$ as a function of γ_1 .

For numerical analysis, Eqs. (4) and (5) can be written in the convenient form:

$$\mathrm{Ln}\left(\frac{\Delta\sigma}{\sigma_0}\right) = \mathrm{Ln}\left\{\gamma\left[\frac{e^2\rho_0}{32\hbar\xi_z(0)}\right]\varepsilon^{-1/2}\right\} \quad (10)$$

$$\mathrm{Ln}\left(\frac{\Delta\sigma}{\sigma_0}\right) = \mathrm{Ln}\left\{\gamma'\left[\frac{e^2\rho_0}{16\hbar d}\right]\varepsilon^{-1}\right\} \quad (11)$$

The logarithmic plot of $\Delta\sigma(T)/\sigma_{room}$ versus $\varepsilon\,[=(T - T_c^{MF})/T_c^{MF}]$ gives the paraconductivity measurement from which we can determine the constant γ_1 numerically with appropriate fitting parameters.

TABLE 1. Experimental parameters of ρ_0, T_c, $\xi_z(0)$, d, T_{exp} for $(ZnO)_x/Bi_{1.8}Pb_{0.4}Sr_2Ca_2Cu_3O_{10+\delta}$ [18] and $(Cu_{0.5}Tl_{0.5-x}Ti_x)Ba_2Ca_2Cu_3O_{10-\delta}$ [19], with $x = 0.0$.

Sample	ρ_0 (mΩ.cm)	T_c (K)	d (Å)	$\xi_z(0)$ (Å)	T_{exp} (K)	T_{est} (K)
(Bi,Pb)-2223 (2D)	0.1678	110.0	129.0	1.06	113.92 <T_{exp}< 131.13	112.92 <T_{est}< 128.37
(Cu,Tl)-1223 (2D, 3D)	0.99	122.9	86.0	5.06	124.9 <T_{exp}< 144.40 124.3 <T_{exp}< 124.90	124.94 <T_{est}< 144.69 124.32 <T_{est}< 124.94

For numerical analysis, we took the experimental results reported by M. Roumié et al. [18] for the $(ZnO)_x$/(Bi,Pb)-2223 phase. They fitted their data to the two-dimensional fluctuation conductivity. We follow their experimental result (Fig. 2), and our new expression (i.e., Eq. (4), corresponding to Eq. (5)) is well fitted with $d = 129$ Å, $\rho_0 = 167.8$ μΩcm and $\gamma' = 2.25$; indicating larger anisotropy in two dimensions.

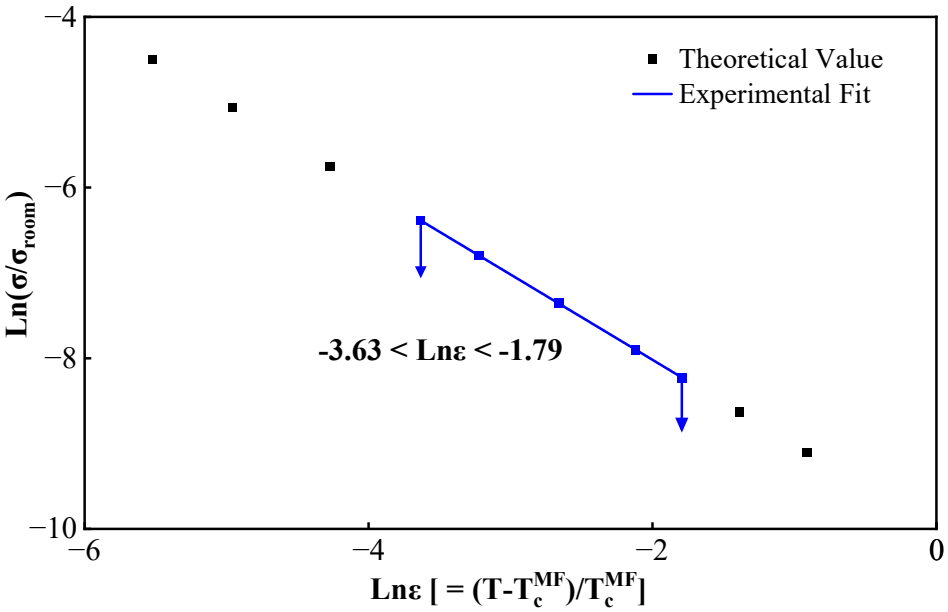

FIG. 2. Double-logarithmic plot of the reduced paraconductivity versus reduced temperature for $(ZnO)_x/Bi_{1.8}Pb_{0.4}Sr_2Ca_2Cu_3O_{10+\delta}$ with $x = 0.0$. The square dots are the theoretical fit, i.e., Eq. (11), and the solid line (marked by arrows) is the experimental fit [18].

We also considered the experimental results reported by N. H. Mohammed et al. [19] for the $(Ti)_x$/(Cu,Tl)-1223 phase, who fitted their data to two-dimensional fluctuation conductivity. We followed their experimental results (Fig. 3) and our new expression is well fitted with d = 86 Å, $\rho_0 = 990$ μΩcm and $\gamma' = 2.12$, indicating larger anisotropy in two dimensions.

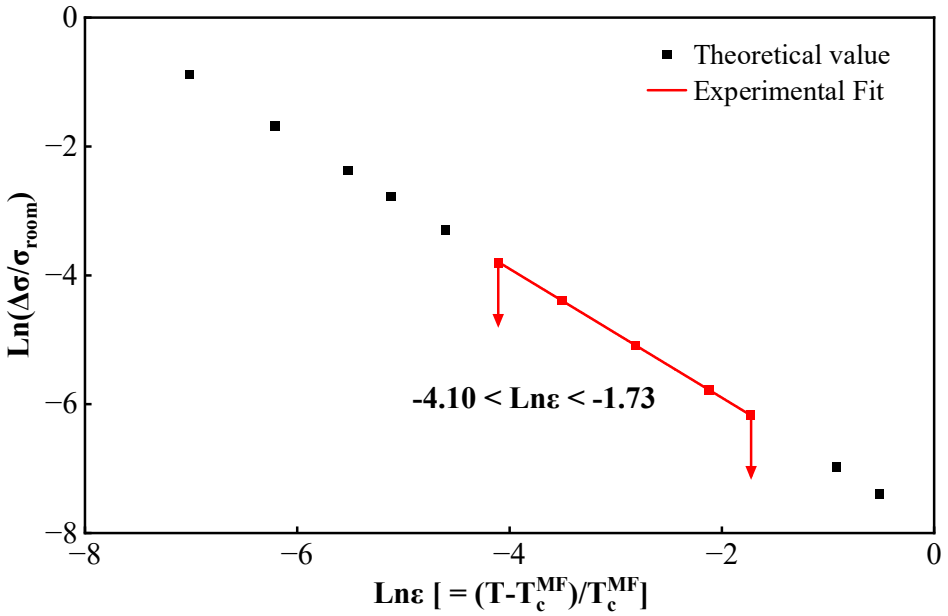

FIG. 3. Double-logarithmic plot of $\Delta\sigma(T)/\sigma_{room}$ versus $\varepsilon\ [= (T - T_c^{MF})/T_c^{MF}]$ for $(Cu_{0.5}Tl_{0.5-x}Ti_x)Ba_2Ca_2Cu_3O_{10-\delta}$ with $x = 0.0$. The square dots are the theoretical fit, i.e., Eq. (11), and the solid line (marked by arrows) is the experimental fit [19].

For three-dimensional paraconductivity, we can reproduce the experimental result reported by N. H. Mohammed et al. [19] for the $(Ti)_x$/(Cu,Tl)-1223 phase and fit our data (within the temperature range indicated by the arrows in Fig. 4) to Eq. (10) by substituting $\xi_z(0) = 5.06$ Å, $\rho_0 = 990$ μΩcm and $\gamma = 0.64$, indicating smaller anisotropy in three dimensions.

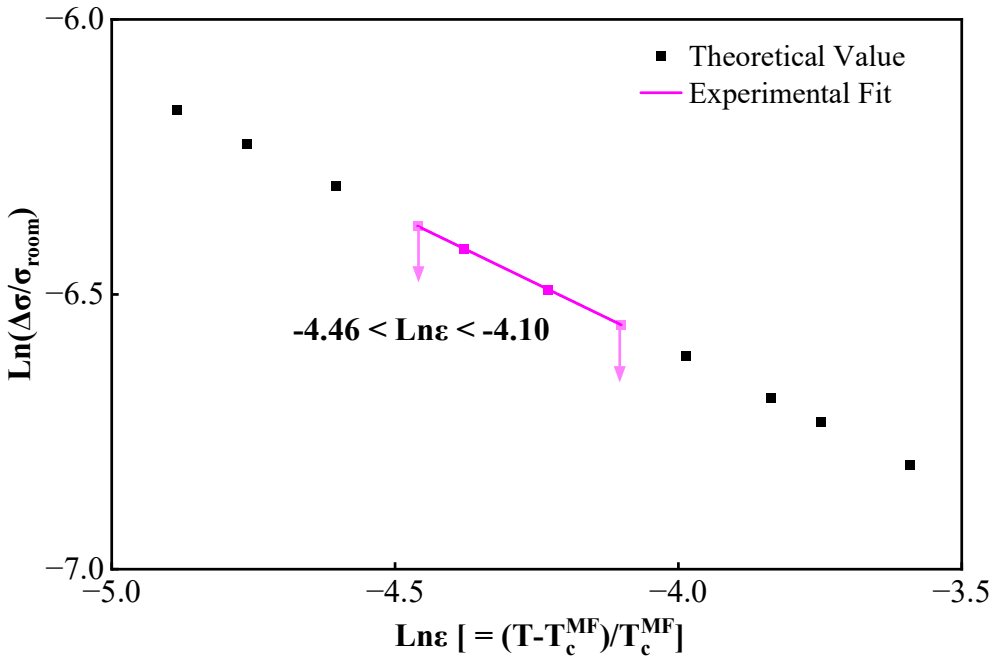

FIG. 4. Double-logarithmic plot of $\Delta\sigma(T)/\sigma_{room}$ versus $\varepsilon\ [=(T-T_c^{MF})/T_c^{MF}]$ for $(Cu_{0.5}Tl_{0.5-x}Ti_x)Ba_2Ca_2Cu_3O_{10-\delta}$ with $x = 0.0$. The square dots are the theoretical fit, i.e., Eq. (10), and the solid line (marked by arrows) is the experimental fit [19].

4. Discussion and Conclusion

In this work, we present a theoretical method to evaluate coherence-length anisotropy in high-temperature superconductors using a fluctuation-enhanced conductivity or paraconductivity approach. Well-established paraconductivity formulations are applied to two representative systems: the ZnO-doped (Bi,Pb)-2223 phase and the Ti-doped (Cu,Tl)-1223 phase, representing two- and three-dimensional structures, respectively. The analysis shows that two-dimensional superconductors exhibit greater anisotropy, whereas three-dimensional samples show relatively lower anisotropy. To verify the theoretical predictions, we employed previously reported parameter values for the selected compounds. The data set was analyzed using a statistical regression model. We have standard errors of 0.49 for (Bi,Pb)-2223 (2D), 0.60 for 2D- and 0.063 for 3D-(Cu,Tl)-1223, respectively. These suggest that the experimental data used here are statistically reliable. In particular, the minimal error observed for the 3D (Cu,Tl)-1223 sample indicates better measurement stability compared with the 2D sample. The results demonstrate good consistency between the theoretical and experimental findings, supporting the validity of the proposed model. Finally, we concluded that the paraconductivity approach is a useful tool for estimating the coherence length anisotropy in High-Temperature SuperConductors (HTSCs).

Acknowledgements

This work was performed in the Physics Department, Faculty of Science, University of Chittagong, Chattogram-4331, Bangladesh. Thanks are due to Prof. Dr. Md. Rafiqul Islam, Head of the Superconductivity Research Group and Chairman, Department of Physics, for providing all kinds of departmental facilities during this research. We gratefully acknowledge Prof. Dr. Ahmad Mohammed Alsaad for his valuable comments and suggestions.

Conflict of interest

The authors declare no conflict of interest.

Funding

The authors received no financial support for the research during the preparation of this manuscript.

Ethical Approval

This article does not contain any studies with human participants or animals performed by any of the authors.

References

[1] Jin, B.Y. and Ketterson, J.B., Adv. Phys., 38 (3) (1989) 189.

[2] Naughton, M.J., Yu, R.C., Davies, P.K., Fischer, J.E., Chamberlin, R.V., Wang, Z.Z., Jing, T.W., Ong, N.P., and Chaikin, P.M., Phys. Rev. B, 38 (13) (1988) 9280.

[3] Kobayashi, N., Hirano, K., Nishizaki, T., Iwasaki, H., Sasaki, T., Awaji, S., Watanabe, K., Asaoka, H., and Takei, H., Physica C, 251 (1995) 255.

[4] Roulin, M., Junod, A., and Walker. E., Physica C 260 (1996) 257.

[5] Blatter, G., Geshkenbein, V.B., and Larkin, A.I., Phys. Rev. Lett. 68 (6) (1992) 875.

[6] Blatter, G., Feigelman, M.V., Geshkenbein, V.B., Larkin, A.I., and Vinokur, V.M., Rev. Mod. Phys., 66 (4) (1994) 1125.

[7] Larbalestier, D., Gurevich, A., Feldmann, D.M., and Polyanskii, A., Nature, 414 (2001) 368.

[8] Maiorov, B., Baily, S.A., Zhou, H., Ugurlu, O., Kennison, J.A., Dowden, P.C., Holesinger, T.G., Foltyn, S.R., and Civale, L., Nat. Mater., 8 (2009) 398.

[9] Sieger, M., Pahlke, P., Lao, M., Eisterer, M., Meledin, A., Tendeloo, G.V., Ottolinger, R., Hanisch, J., Holzapfel, B., Usoskin, A., Kursumovic, A., MacManus-Driscoll, J.L., Stafford, B.H., Bauer, M., Nielsch, K., Schultz, L., and Huhne, R., IEEE Trans. Appl. Supercond., 27 (8) (2017).

[10] Sedky, A. and Mohamed, S.B., Chin. Phys. B, 22 (11) (2013) 117401.

[11] Gurevich, A., Rep. Prog. Phys., 74 (11) (2011) 124501.

[12] Hosono, H., Yamamoto, A., Hiramatsu, H., and Ma, Y., Mater. Today, 21 (3) (2018) 278.

[13] Sun, Y., Pan, Y., Zhou, N., Xing, X., Shi, Z., Wang, J., Zhu, Z., Sugimoto, A., Ekino, T., Tamegai, T., and Kitano, H., Phys. Rev. B, 103 (22) (2021) 224506.

[14] Aslamazov, L.G. and Larkin, A.I., Phys. Lett. A, 26 (6) (1968) 238.

[15] Hofengärtner, R., Hensel, B., and Saemann-Ischenko, B., Phys. Rev. B, 44 (2) (1991) 741.

[16] Islam, M.R., Bangladesh J. Phys., 3 (2006) 23.

[17] Gradshleyn, I.S. and Ryzhik, I.M., “Table of Interals Series and Products”, (Academic press, New York, London, 1965), p-295.

[18] Roumié, M., Abdeen, W., Awad, R., Korek, M., Hassan, I., and Mawassi, R., J. Low Temp. Phys., 174 (2014) 45.

[19] Mohammed, N.H., Physica C, 485 (2013) 95.